Iranian Journal of Materials Forming 6 (1) (2019) 64-73

Online ISSN: 2383-0042

IJMF

Iranian Journal of Materials Forming

Journal Homepage: http://ijmf.shirazu.ac.ir

Modeling of Corrosion-Fatigue Crack Growth Rate Based on Least Square Support Vector Machine Technique

N. Anjabin* and F. Arabloo

Department of Materials Science and Engineering, School of Engineering , Shiraz University, Shiraz, Iran

ARTICLE INFO

Article history:

Received 19 November 2018
Revised 31 March 2019
Accepted 16 April 2019

Keywords:

Corrosion-fatigue crack growth
Modeling
LSSVM
Ti-6A1-4V
HSLA steel.

ABSTRACT

Understanding crack growth behavior in engineering components subjected to cyclic fatigue loadings is necessary for design and maintenance purpose. Fatigue crack growth (FCG) rate strongly depends on the applied loading characteristics in a nonlinear manner, and when the mechanical loadings combine with environmental attacks, this dependency will be more complicated. Since, the experimental investigation of FCG behavior under various loading and environmental conditions is time-consuming and expensive, applying a reliable methodology for prediction of this property is essential. In this regard, a modeling technique based on least square support vector machine (LSSVM) framework is employed for prediction of FCG behavior of three different alloys including, Ti-6Al-4V alloy and two Cu-strengthened high strength low alloy (HSLA) steels in the air and corrosive media. The parameters of the developed model were calculated employing the coupled simulated annealing optimization technique. The performance and accuracy of the developed models were tested and validated by their ability to predict the experimental data. Statistical error analyses indicated that the developed model can satisfactorily represent the experimental data with high accuracy.

1. Introduction

Fatigue life assessment of structural components operating under fluctuating loads has a great significance in the reliability of these components [1-3]. The progressive damage induced by fatigue loading is characterized by two steps of crack nucleation and crack propagation [4]. Different theoretical models have been proposed to describe the process of fatigue failure, which can be categorized into the continuous damage mechanics (CDM) and the fracture mechanics (FM) approaches [1, 3, 5]. In the CDM approach, a damage evolution rule is used along with a stress/strain criterion to predict the damage accumulation, and nucleation of a detectable crack in a structure [2, 4-6], while the FM approach is suited for materials containing initial crack-like defect of known sizes and locations [5]. In this method, the fatigue life is predicted by computing the propagation of a pre-existing crack from an initial size to a critical value, where instability occurs [2, 7]. The FM method which relies on the fatigue crack growth (FCG) is widely accepted and used for fatigue life predictions in different engineering components [1-3]. Normally the crack growth rate ($\frac{da}{dN}$) is related to the stress intensity factor range (Δk), and the corresponding curve is known as the FCG curve [3, 6, 8]. In the logarithmic scale, the FCG curve can be divided into three regions, the near-threshold region, the middle region which corresponds to the stable crack growth, and unstable crack propagation region just prior to final failure [9, 10].

The most famous equation used for the FCG curve modeling was introduced by Paris and Erdogan in 1963.

* Corresponding author
E-mail addresses: Anjabin@shirazu.ac.ir (N. Anjabin)

This empirical power law equation is only suited for the intermediate region of the FCG curve, and assume a linear behavior in the logarithmic scale [8, 9, 11]. However, the experimental investigations show that the relationships between $\log(\frac{da}{dN})$ and $\log(\Delta k)$ are not linear even in the intermediate region [10]. Moreover, it is observed that the FCG curve is strongly influenced by the stress ratio [9], which is ignored in Paris' law. In the literature, there are many empirical equations for the prediction of the FCG rate by modifying the original Paris' law to take account of the influences of the stress ratio, such as Walker's law [3, 9-12]. However, these modified models are only applicable for the intermediate region of the FCG curve, and does not account for the unstable crack growth regions. In order to describe the whole regions of the crack growth curve, different nonlinear relationships between the logarithm of the crack growth rate and the logarithm of the stress intensity factor range were proposed such as Forman's law, the hyperbolic sine law, sigmoidal equation, and cubic polynomial approximation [10, 12]. It is clearly indicated that the fatigue crack growth can also be affected by the environment [10]. In addition to the stress intensity factor range, and the stress ratio, in an aggressive environment, the frequency of the applied load, which represents the time for an environmental attack, may also affect the rate of the crack growth [1, 10]. The above-mentioned models can be used for the FCG in corrosive media by fitting the model predictions to the experimental data for a given environment and loading frequency [10]. However, due to the various factors affecting the FCG behavior of materials, and their interrelationships, there are not any general and explicit formulas to describe the FCG behavior. Alternatively, different machine learning algorithms, which use statistical techniques and experimental data to train the model, were employed in fatigue studies. Pidaparti and Palakal [13] used a back-propagation neural network method to model the FCG behavior of AA7075 aluminum alloy under different types of aircraft spectrum loadings. Mohanty et al [14] and Zhang et al [15] utilized the artificial neural network (ANN) method to model the fatigue crack propagation life for different aluminum alloys. Wang et al [16] used three different ANN algorithms, including extreme learning machine, radial basis function network and genetic algorithms to optimize the back propagation network for the fatigue crack growth calculations. The results indicate that the applied model can successfully predict the nonlinearities of the fatigue crack growth rate. Hong et al [17] presented a support vector regression (SVR) method to predict the fatigue life of laminated composite materials. Song et al [18] applied the extended finite element method (XFEM) and SVR to predict the fatigue life of a plate structure. Mohanty et al [19] used the genetic programming approach for the fatigue life prediction of AA2024 aluminum alloy with reasonable accuracy. However, there are only a few attempts at predicting the environmental effects on the FCG behavior by applying the ANN method. Cheng et al [20] proposed an ANN model for the on-line corrosion fatigue crack growth (CFCG) monitoring of an austenitic stainless steel in a NaCl solution at the loading ratio of 0.3 and different loading frequencies. Haque and Sudhakar [21] analyzed the CFCG of a dual phase steel with various martensite contents between 32 and 76%, in a 3.5% NaCl solution using an ANN-based model. Although these modeling results were found to be in good congruence with the experimental data, the effects of different environments and loading ratios on the CFCG were not considered.

Hence in the present study, for the first time, an approach based on the least square version of the support vector machine was designed to model the CFCG behavior of Ti-6Al-4V alloy and two different types of HSLA steels, when they are exposed to different cyclic loadings in the environments containing different levels of NaCl.

2. LSSVM Background and Modeling

The support vector machine (SVM) is a powerful learning technique, extensively utilized for classification and regression studies [22-29]. SVM-based models have many advantages over the traditional ANN models. In order to construct an ANN model, it is needed to set various parameters such as the number of hidden layers and nodes and the types of activation and training functions, which are usually done in a trial and error manner [30-34]. Also, the bias and weight terms of the

ANN models are usually selected using a gradient-based optimization technique which may converge to a local minimum point instead of the global solution [30-34]. In contrast to the ANN-based methods, the SVM models have fewer adjustable parameters and usually converge toward the global solution [26]. However, in the SVM approach, a large-scale problem with nonlinear programming should be solved [35]. In order to overcome this difficulty, a modified version of the standard SVM, known as LSSVM, was introduced which uses linear programming instead of solving quadratic problems [22, 36, 37]. In the LSSVM formulation, the following function is used to predict the output data (y_k) from the input data points ($\boldsymbol{x_k}$).

$$y_k = \langle \boldsymbol{w}, \Phi(\boldsymbol{x_k})\rangle + b \qquad k = 1,\dots,N \tag{1}$$

Where $\boldsymbol{x_k}$ stands for the input vectors, y_k for scaler output values, N is the number of input data set, <.,.> represent dot product, $\Phi(\boldsymbol{x_k})$ is the nonlinear function that was used to map the input data from R^n into a space with higher dimension, and b and $\boldsymbol{w}$ are bias term and weight vector, respectively. To calculate the values of b and $\boldsymbol{w}$, the following objective function needs to be minimized [35, 38]:

$$L_{LS-SVM} = \frac{1}{2}\|\boldsymbol{w}\|^2 + \frac{1}{2}\gamma \sum_{k=1}^{N} e_k^2 - \sum_{k=1}^{N} \alpha_k\{e_k + \langle \boldsymbol{w}, \Phi(\boldsymbol{x_k})\rangle + b - y_k\} \qquad k = 1,\dots,N \tag{2}$$

where, γ, e_k, and α_k are regularization constant, error variables, and Lagrange multipliers, respectively. Differentiation of Eq. (2) with respect to $\boldsymbol{w}$, b, e_k and α_k, leads to [35, 38]:

$$\begin{cases} \frac{\partial L_{LS-SVM}}{\partial w} = 0 \rightarrow \boldsymbol{w} = \sum_{k=1}^{N} \alpha_k \Phi(\boldsymbol{x_k}) \\ \frac{\partial L_{LS-SVM}}{\partial b} = 0 \rightarrow \sum_{k=1}^{N} \alpha_k = 0 \\ \frac{\partial L_{LS-SVM}}{\partial e_k} = 0 \rightarrow \alpha_k = \gamma\, e_k \\ \frac{\partial L_{LS-SVM}}{\partial \alpha_k} = 0 \rightarrow \langle \boldsymbol{w}, \Phi(\boldsymbol{x_k})\rangle + b + e_k - y_k = 0 \end{cases} \tag{3}$$

Eq. (3) can be rewritten as [35];

$$\begin{bmatrix} 0 & \boldsymbol{1}_N^T \\ \boldsymbol{1}_N & \Omega + \gamma^{-1}\boldsymbol{I}_N \end{bmatrix} \begin{bmatrix} b \\ \boldsymbol{\alpha} \end{bmatrix} = \begin{bmatrix} 0 \\ \boldsymbol{Y} \end{bmatrix} \tag{4}$$

where $\boldsymbol{1}_N = [1,\dots,1]^T$, $\boldsymbol{Y} = [y_1,\dots,y_N]^T$, $\boldsymbol{\alpha} = [\alpha_1,\dots,\alpha_N]^T$, $\boldsymbol{I}_N$ is the $N\times N$ identity matrix and Ω is the kernel matrix:

$$\Omega_{lk} = \Phi(\boldsymbol{x_l})^T \Phi(\boldsymbol{x_k}) \quad l,k = 1,\dots,N \tag{5}$$

3. Data Acquisition and Processing

3.1. Pre-processing

Experimental data reported for the CFCG behavior of Ti-6Al-4V alloy and two types of HSLA steels (Table 1) were used in the present study [10, 39].

Table 1. Chemical composition of HSLA steels [39].

Steel	C	Mn	Si	Cr	Mo	Ni	Cu
HSLA-80	0.05	1.00	0.34	0.61	0.51	1.77	1.23
HSLA-100	0.06	0.84	0.25	0.74	0.58	3.47	1.54

These data describe the CFCG behavior of the alloys in environments with different concentrations of NaCl (0-3.5 wt. %), under various stress ratios (0.1, 0.4, 0.5, and 0.7) and loading frequencies (0.1, 1, 5, and 10 HZ). For the modeling purpose, four independent variables, including the stress intensity factor range (ΔK), NaCl content, stress ratio (R) and loading frequency were selected as input parameters and the CFCG rate was taken as the target (output) variable. The experimental data were divided into two datasets, including the training set and the testing set. For this purpose, 2/3 of the experimental data for each alloy were assigned to the training set, and the remaining was applied to the testing set. In order to have a better distribution of the data on the problem domain, the data assignment process was repeated several times.

3.2. Designing the LSSVM model for CFCG rate prediction

To develop the LSSVM models to predict the CFCG rate, the following relationship was assumed:

$$log(\,CFCG\ rate) = f(log(\,\Delta K), R, Freq, NaCl\%) \tag{6}$$

During the computation, the radial basis function (RBF) is used as a kernel function, which has the following general form [40-42].

$$\Omega_{lk} = exp(-\|x_l - x_k\|^2/\sigma^2) \tag{7}$$

Where σ is a decision variable. In the LSSVM modeling, σ^2 and γ parameters are determined using the optimization calculations. To do so, the mean square error (MSE) between the desired and predicted output values, as defined by Eq. (8), is considered as an objective function.

$$MSE = \frac{1}{N}\sum_i (d_i - p_i)^2 \tag{8}$$

Where, d and p are the target and predicted values, respectively.

4. Results and Disscusion

The values of the LSSVM parameters, including γ and σ^2, were determined by employing the coupled simulated annealing (CSA) [43] technique, and the optimized values are presented in table 2. Simulated annealing (SA) is a probabilistic optimization method inspired by the thermodynamic annealing process of metals.

Table 2. Values of LSSVM parameters determined by CSA optimization method.

Parameter	Ti-6Al-4V	HSLA-80	HSLA-100
σ^2	0.1029	3.0221	1.8701
γ	1.64×10^4	1.056×10^4	722.86

SA technique is widely used in the optimization problems, due to its ability to find the global optimum. However, this optimizer is very sensitive to the initialization parameters, which needs the evaluation of the cost function for several times. In order to reduce the sensitivity of the SA method to the initialization condition, the CSA optimization method was introduced [43]. In CSA, several SA optimizers work together and the information of the current state energy of each optimizer is exchanged with others, which results in a global optimization technique with low sensitivity to the initialization parameters. More detailed discussions about the CSA are reported in [43]. In Figs. 1 through 3, the effects of the stress ratio (R- ratio) on the FCG rate in the air and corrosive media are depicted for Ti-6Al-4V, HSLA-80, and HSLA-100 alloys, respectively. In these figures, the experimental data (symbols) which have been obtained from the published literature [10, 39], are presented along with the corresponding LSSVM model predictions (solid lines).

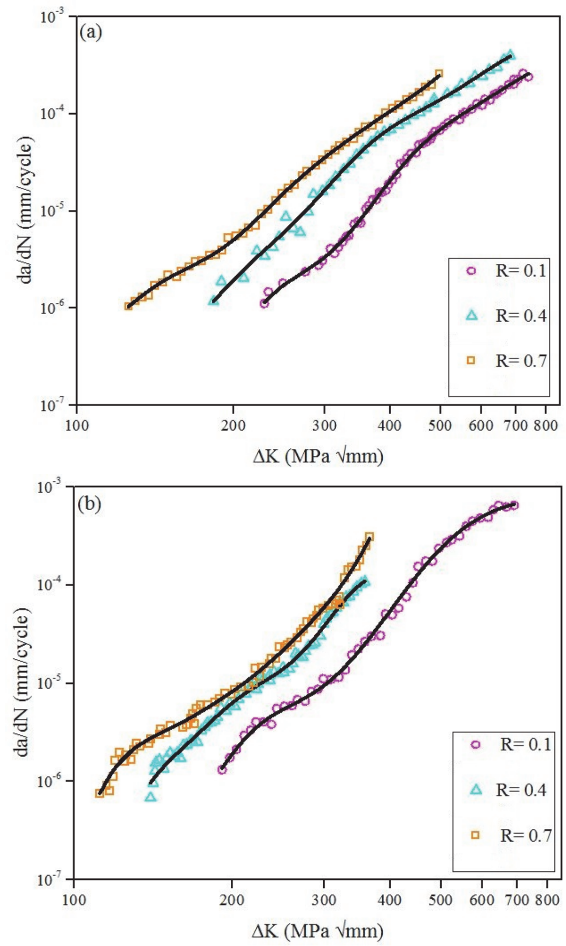

Fig. 1. The effect of stress ratio on FCG behavior of Ti-6Al-4V alloy at different environments (a) air (b) 1% NaCl solution (symbols: experimental data [10]; solid lines: LSSVM predictions).

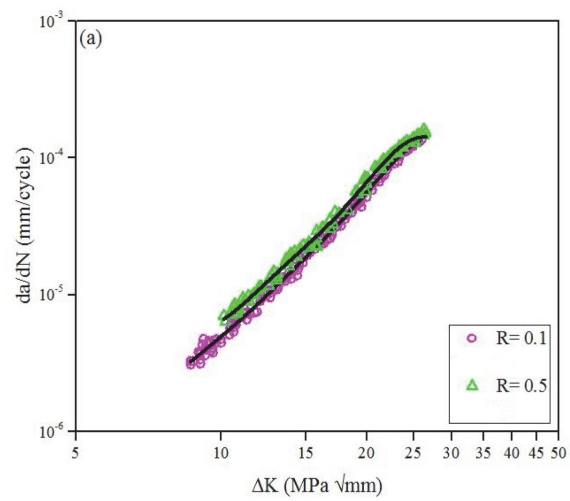

Fig. 2. The effect of stress ratio on FCG behavior of HSLA-80 alloy at different environments (a) air (b) 3.5 % NaCl solution (symbols: experimental data [39]; solid lines: LSSVM predictions).

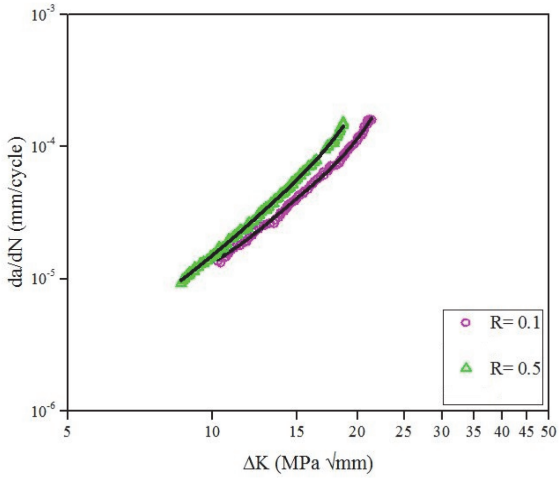

Fig. 2. Continue

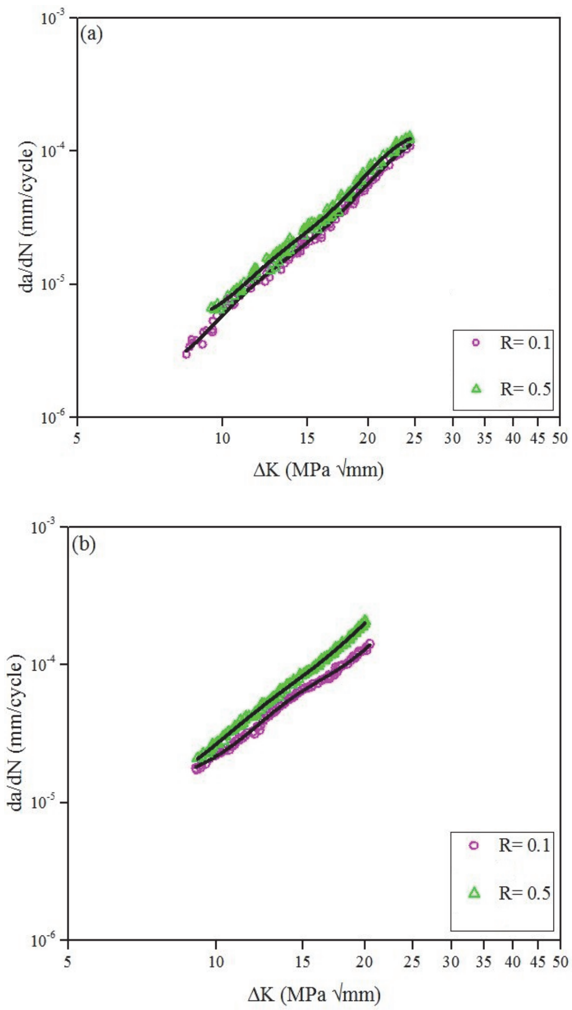

Fig. 3. The effect of stress ratio on FCG behavior of HSLA-100 alloy at different environments (a) air (b) 3.5 % NaCl solution (symbols: experimental data [39]; solid lines: LSSVM predictions).

As could be seen from Figs. 1-3, the FCG rate at a given stress ratio is enhanced by exposing the samples to the corrosive media. Also, it is evident that by increasing the R-ratio the FCG rate is increased in both air and corrosive media. This behavior was rationalized by the increased crack closure observed at low R-ratios [39, 44, 45]. In the presence of the crack closure, the crack growth rate is governed by the effective stress intensity factor range ($\Delta K_{eff} = K_{max} - K_{open}$) instead of $\Delta K = K_{max} - K_{min}$, where K_{open} has higher values than K_{min}. However, at higher R-ratios, the crack closure effects disappear; hence the FCG rate at higher R-ratios is expected to be higher than that of lower R-ratios. By increasing the R-ratios, the increment in the FCG rates, is more pronounced for the samples placed in the corrosive environment than the samples tested in the air. This observation is rationalized by the increased effects of the crack closure in the corrosive media. According to Figs. 1-3, the proposed model can well predict the nonlinear nature of the FCG curve at different stress ratios and environmental conditions. In Figs. 4 and 5, the influences of the test frequency on the CFCG rate for Ti-6Al-4V, and HSLA steels are depicted, respectively.

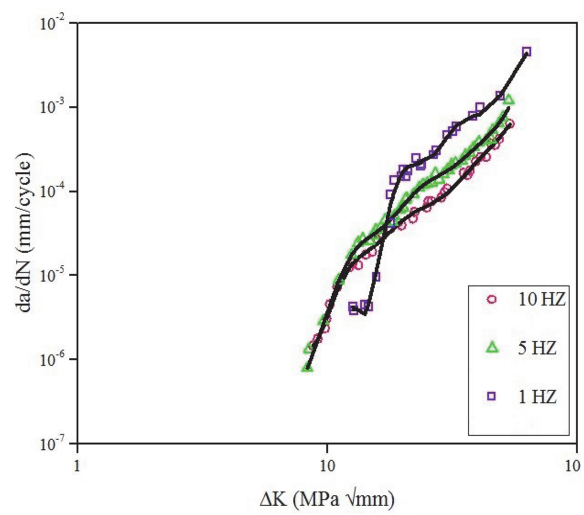

Fig. 4. The effect of load frequencies on FCG behavior of Ti-6Al-4V alloy at 3.5 % NaCl solution (symbols: experimental data [10]; solid lines: model predictions).

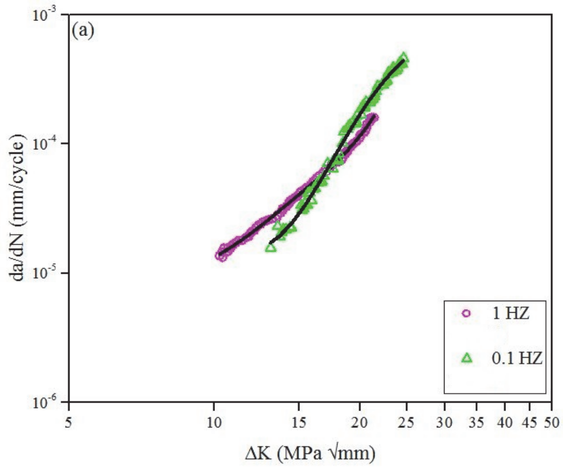

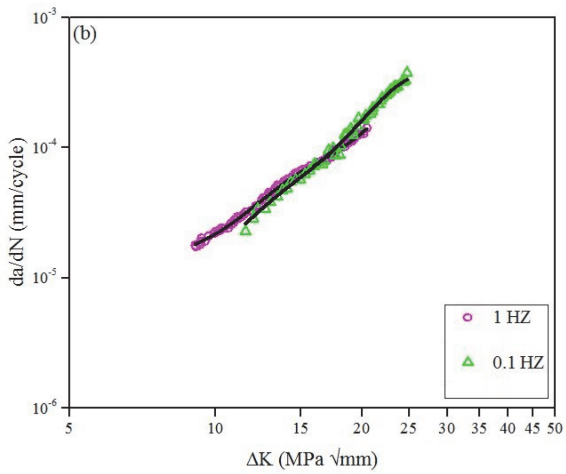

Fig. 5. The effect of load frequencies on FCG behavior in 3.5 % NaCl solution, for (a) HSLA-80, and (b) HSLA-100 alloy (symbols: experimental data [39]; solid lines: model predictions).

According to Figs. 4 and 5, the CFCG rate will change significantly with the loading frequency. As seen in these figures, there is a critical value for ΔK in which by decreasing the frequency, the CFCG rate decreases below this limit, and increases above it. This behavior can be related to a possible change in the crack growth mechanism by making changes in the loading frequency and ΔK values [39]. Hence the prediction of the CFCG behavior is a relatively difficult task. As obviously seen in Figs. 4 and 5, the developed model can successfully predict the CFCG behavior of the alloys considered here at different loading frequencies. Tables 3-5 indicate the statistical parameters of the proposed LSSVM model to predict the corrosion–fatigue behavior of the alloys in the air and corrosive (NaCl solution) environment. These statistical parameters include average relative deviation (ARD), average absolute relative deviation (AARD), and root mean square error (RMSE), as defined bellow;

$$ARD\ \% = \frac{100}{N}\sum_{i=1}^{N}\left(\frac{Y_i^{exp}-Y_i^{pred}}{Y_i^{exp}}\right) \tag{9}$$

$$AARD\ \% = \frac{100}{N}\sum_{i=1}^{N}\left(\left|\frac{Y_i^{exp}-Y_i^{pred}}{Y_i^{exp}}\right|\right) \tag{10}$$

$$RMSE = \left(\frac{\sum_{i=1}^{N}\left(Y_i^{exp}-Y_i^{pred}\right)^2}{N}\right)^{\frac{1}{2}} \tag{11}$$

Table 3. The statistical parameters of the proposed LSSVM model for Ti-6Al-4V alloy.

Parameters	Values		
	Training set	Test set	Total
Average relative deviation, %	-0.45	-0.80	-0.44
Average absolute relative deviation , %	6.29	8.42	6.97
Root mean square error	9.25×10^{-6}	3.6×10^{-5}	2.26×10^{-5}
Number of data points	272	146	418

Table 4. The statistical parameters of the proposed LSSVM model for HSLA-80 alloy.

Parameters	Values		
	Training set	Test set	Total
Average relative deviation, %	-0.14	-0.064	-0.11
Average absolute relative deviation , %	3.89	4.44	4.08
Root mean square error	4.6×10^{-6}	3.87×10^{-6}	4.36×10^{-6}
Number of data points	298	160	458

Table 5. The statistical parameters of the proposed LSSVM model for HSLA-100 alloy.

Parameters	Values		
	Training set	Test set	Total
Average relative deviation, %	-0.12	-0.69	- 0.38
Average absolute relative deviation , %	3.64	1.79	1.97
Root mean square error	2.88×10^{-6}	4.68×10^{-6}	3.61×10^{-6}
Number of data points	265	143	408

where Y_i^{exp} and Y_i^{pred} are the experimental data and the corresponding predicted values. According to these tables, the developed model can predict the corrosion–fatigue behavior of the considered alloys with a very low prediction error. For a better illustration of the degree of the agreement between the predicted values by the LSSVM models and the experimental data, the model's results for each alloy are plotted against the experimental (target) data in Figs. 6-8. From these figures, all the data points lie tightly around the 45° line which indicates the accuracy and robustness of the developed models.

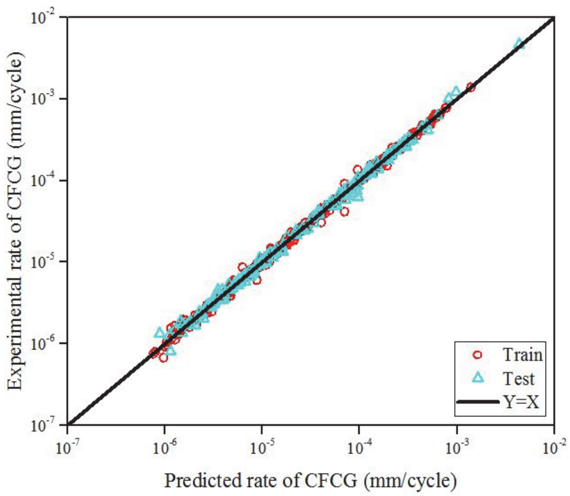

Fig. 6. Comparison between the predicted results of the developed LSSVM models and the experimental data for CFCG behavior of Ti-6Al-4V alloy.

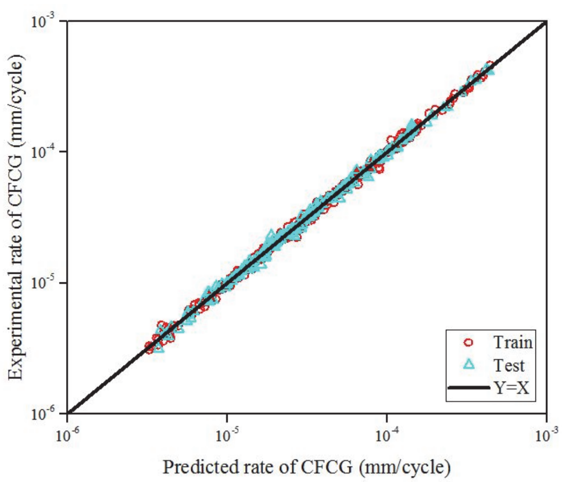

Fig. 7. Comparison between the predicted results of the developed LSSVM models and the experimental data for CFCG behavior of HSLA-80 alloy.

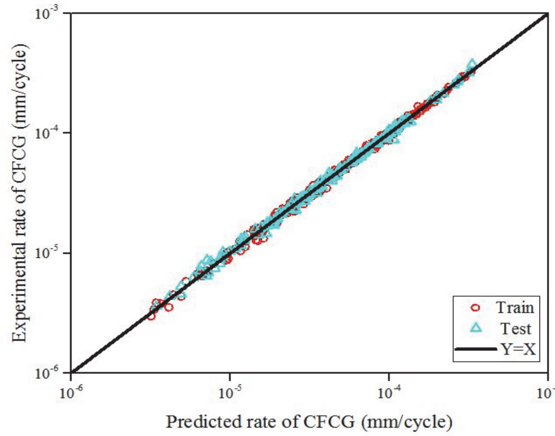

Fig. 8. Comparison between the predicted results of the developed LSSVM models and the experimental data for CFCG behavior of HSLA-100 alloy.

5. Conclusions

The present study focused on the application of the LSSVM intelligent modeling approach for accurate prediction of the FCG rate of three different alloys, Ti-6Al-4V, and two HSLA steels, in the air and corrosive environments. The experimental data reported in the published literature were used to construct the model. The parameters of the developed model were optimized using the coupled simulated annealing method. The proposed LSSVM method was successfully employed to predict the corrosion-fatigue crack growth behavior of the alloys at different loading frequencies and stress ratios. The performance and usefulness of the LSSVM modeling approach to estimate the fatigue crack growth rate were shown by various statistical parameters, and graphical evaluations, which indicates that there is high accordance between the experimental data and the predicted results.

6. References

[1] R. Ghosh, Remaining life assessment of engineering components, Recent Trends in Structural Integrity Assessment, *National Metallurgical Laboratory*, *India* (2001) pp. 1-17.

[2] E. Santecchia, A. Hamouda, F. Musharavati, E. Zalnezhad, M. Cabibbo, M.E. Mehtedi, S. Spigarelli, A review on fatigue life prediction methods for metals, *Advances in Materials Science and Engineering* (2016) 1-26.

[3] W. Zhang, H. Liu, Q. Wang, J.J.M. He, A fatigue life prediction method based on strain intensity factor, *Materials* 10 (7) (2017) 689.

[4] R. Brighenti, A. Carpinteri, N. J. Corbari, Damage mechanics and Paris regime in fatigue life assessment of metals, *International Journal of Pressure Vessels and Piping* 104 (2013) 57-68.

[5] J. Mazars, G. Pijaudier-Cabot, From damage to fracture mechanics and conversely: a combined approach, *International Journal of Solids and Structures* 33 (20-22) (1996) 3327-3342.

[6] V. Shenoy, I.A. Ashcroft, G.W. Critchlow, A.D. Crocombe, Fracture mechanics and damage mechanics based fatigue lifetime prediction of adhesively bonded joints subjected to variable amplitude fatigue, *Engineering Fracture Mechanics* 77 (7) (2010) 1073-1090.

[7] G. C. Sih, E.T. Moyer Jr, Path dependent nature of fatigue crack growth, Engineering Fracture Mechanics 17 (3) (1983) 269-280.

[8] Ž. Božić, S. Schmauder, M. Mlikota, Fatigue growth models for multiple long cracks in plates under cyclic tension based on ΔK_I, ΔJ-integral and ΔCTOD parameter, *Key Engineering Materials* 488 (2012) 525-528.

[9] A. F. Siqueira, C.A.R.P. Baptista, O.L.C. Guimarães, C.O.F.T. Ruckert, Describing the total fatigue crack growth curves for aluminum alloys with an exponential equation, *Procedia Engineering* 2 (1) (2010) 1905-1914.

[10] E. Richey III, A.W. Wilson, J.M. Pope, R.P. Gangloff, Computer modeling the fatigue crack growth rate behavior of metals in corrosive environments, *NASA Contractor Report 194982, Virginia* (1994).

[11] T. T. Shih, R.P. Wei, A study of crack closure in fatigue, *Engineering Fracture Mechanics* 6 (1) (1974) 19-32.

[12] C. Proppe and G. Schuëller, Stochastic analysis of fatigue crack growth, *In ICF10, Honolulu, USA* (2001).

[13] R. M.V. Pidaparti and M.J. Palakal, Neural network approach to fatigue-crack-growth predictions under aircraft spectrum loadings, *Journal of Aircraft* 32 (4) (1995) 825-831.

[14] J. Mohanty, B. Verma, D. Parhi, P. Ray, Application of Artificial Neural Network for Predicting Fatigue Crack Propagation Life of Aluminum Alloys, *Association of Computational Materials Science and Surface Engineering* 1 (2009) 133.

[15] W. Zhang, Z. Bao, S. Jiang, J. He, An Artificial Neural Network-Based Algorithm for Evaluation of Fatigue Crack Propagation Considering Nonlinear Damage Accumulation, Materials 9 (6) (2016) 483.

[16] H. Wang, W. Zhang, F. Sun, W.J.M. Zhang, A Comparison Study of Machine Learning Based Algorithms for Fatigue Crack Growth Calculation, *Materials* 10 (5) (2017) 543.

[17] W. C. Hong, F.M. Lai, J.H. Wu, P.F. Pai, S.L. Yang, Feasibility Assessment of Support Vector Regression Models with Immune Algorithms in Predicting Fatigue Life of Composites, *In Join Conference on Information Sciences, Taiwan* (2006) 1220.

[18] W. Song, Z. Jiang, H. Jiang, Predict the fatigue life of crack based on extended finite element method and SVR, *In AIP Conference Proceedings* 1967 (1) (2018) 30024.

[19] J. Mohanty, T. Mahanta, A. Mohanty, D. N. Thatoi, Prediction of constant amplitude fatigue crack growth life of 2024 T3 Al alloy with R-ratio effect by GP, *Applied Soft Computing* 26 (2015) 428-434.

[20] Y. Cheng, W. Huang, C.J. Zhou, Artificial neural network technology for the data processing of on-line corrosion fatigue crack growth monitoring, *International Journal of Pressure Vessels and Piping* 76 (2) (1999) 113-116.

[21] M. E. Haque, K. J. Sudhakar, Prediction of corrosion–fatigue behavior of DP steel through artificial neural network, *International Journal of Fatigue* 23 (1) (2001) 1-4.

[22] J. A. K. Suykens, J. Vandewalle, Least Squares Support Vector Machine Classifiers, *Neural Processing Letters* 9 (3) (1999) 293-300.

[23] C. Cortes, V. Vapnik, Support-vector networks, *Mach Learn* 20 (3) (1995) 273-297.

[24] V. Vapnik, The Nature of Statistical Learning Theory, *Springer* (2000).

[25] A. Baylar, D. Hanbay, M. Batan, Application of least square support vector machines in the prediction of aeration performance of plunging overfall jets from weirs, *Expert Systems with Applications* 36 (4) (2009) 8368- 8374.

[26] S. Rafiee-Taghanaki, M. Arabloo, A. Chamkalani, M. Amani, M.H. Zargari, M.R. Adelzadeh, Implementation of SVM framework to estimate PVT properties of reservoir oil, *Fluid Phase Equilibria* 346 (2013) 25-32.

[27] E. D. Übeyli˙, Least squares support vector machine employing model-based methods coefficients for analysis of EEG signals, *Expert Systems with Applications* 37 (1) (2010) 233-239.

[28] S. R. Amendolia, G. Cossu, M. L. Ganadu, B. Golosio, G. L. Masala, G.M. Mura, A comparative study of K-Nearest Neighbour, Support Vector Machine and Multi-Layer Perceptron for Thalassemia screening, *Chemometrics and Intelligent Laboratory Systems* 69 (1-2) (2003) 13-20.

[29] T. S. Chen, J. Chen, Y.C. Lin, Y.C. Tsai, Y.H. Kao, K. Wu, A Novel Knowledge Protection Technique Base on Support Vector Machine Model for Anti-classification, *In Zhu M (ed) Electrical Engineering and Control, Lecture Notes in Electrical Engineering, Springer Berlin Heidelberg* (2011) 517-524.

[30] Y. F. Zhang, J.Y.H. Fuh, A Neural Network Approach for Early Cost Estimation of Packing Products, *Computers & Industrial Engineering* 34 (2) (1998) 433-450.

[31] S. Deng, T.H. Yeh, Applying least squares support vector machines to the airframe wing-box structural design cost estimation, *Expert Systems with Applications* 37 (12) (2010) 8417-8423.

[32] J. Bode, Decision support with neural networks in the management of research and development: Concepts and application to cost estimation, *Information and Management* 34 (1) (1998) 33-40.

[33] B. Verlinden, J.R. Duflou, P. Collin, D. Cattrysse, Cost estimation for sheet metal parts using multiple regression and artificial neural networks: A case study, *International Journal of Production Economics* 111 (2) (2008) 484-492.

[34] K. S. Shin, T.S. Lee, H.J. Kim, An application of support vector machines in bankruptcy prediction model, *Expert Systems with Applications* 28 (1) (2005) 127-135.

[35] J. A. K. Suykens, T. Van Gestel, J. De Brabanter, B. De Moor, J. Vandewalle, Least Squares Support Vector Machines, *World Scientific Publishing Co Pte Ltd, Singapor* (2002).

[36] M. M. Ghiasi, A. Shahdi, P. Barati, M. Arabloo, Robust Modeling Approach for Estimation of Compressibility Factor in Retrograde Gas Condensate Systems, *Industrial & Engineering Chemistry Research* 53 (32) (2014) 12872-12887.

[37] N. M. Mahmoodi, M. Arabloo, J. Abdi, Laccase immobilized manganese ferrite nanoparticle: Synthesis and LSSVM intelligent modeling of decolorization, *Water Research* 67 (2014) 216-226.

[38] H. Wang, D. Hu, Comparison of SVM and LS-SVM for regression, *In International Conference on Neural Networks and Brain, Beijing, China* (2005) 279-283.

[39] S. Sivaprasad, S. Tarafder, V. Ranganath, M. Tarafder, K.J. Ray, Corrosion fatigue crack growth behaviour of naval steels, *Corrosion Science* 48 (8) (2006) 1996-2013.

[40] M. Arabloo, A. Shokrollahi, F. Gharagheizi, A.H. Mohammadi, Toward a predictive model for estimating dew point pressure in gas condensate systems, *Fuel Processing Technology* 116 (2013) 317-324.

[41] A. Farasat, A. Shokrollahi, M. Arabloo, F. Gharagheizi, A. H. Mohammadi, Toward an intelligent approach for determination of saturation pressure of crude oil, *Fuel Processing Technology* 115 (2013) 201-2014.

[42] A. Eslamimanesh, F. Gharagheizi, A.H. Mohammadi, D. Richon, Phase Equilibrium Modeling of Structure H Clathrate Hydrates of Methane + Water "Insoluble" Hydrocarbon Promoter Using QSPR Molecular Approach, J. *Journal of Chemical & Engineering Data* 56 (10) (2011) 3775-3793.

[43] S. Xavier-de-Souza, J.A. Suykens, J. Vandewalle, D. Bollé, Coupled simulated annealing, *IEEE Transactions on Systems, Man, and Cybernetics* 40 (2) (2010) 320-335.

[44] H. Masuda, S. Matsuoka, The mechanism of corrosion fatigue crack propagation in structural steels under variable loading, *Corrosion Science* 30 (6–7) (1990) 631-642.

[45] M. Fonte, S. Stanzl-Tschegg, B. Holper, E. Tschegg, A.K. Vasudevan, The microstructure and environment influence on fatigue crack growth in 7049 aluminum alloy at different load ratios, *International Journal of Fatigue* 23 (2001) 311-317.

مدلسازی نرخ رشد ترک خستگی – خوردگی با استفاده از روش حداقل مربعات ماشین بردار پشتیبان

نوذر انجبین، فرخنده عربلو

دانشکده مهندسی، بخش مهندسی مواد، دانشگاه شیراز، شیراز، ایران.

چکیـــده

شناخت رفتار رشد ترک در قطعات مهندسی تحت بارهای متناوب خستگی، برای اهداف طراحی و تعمیر و نگهداری ضروری می باشد. نرخ رشد ترک خستگی (FCG) به میزان زیادی به مشخصات بار اعمالی بستگی دارد که این وابستگی اغلب به‌صورت غیرخطی است. چنانچه بارهای مکانیکی با حملات محیطی همراه شود این وابستگی پیچیده‌تر می‌شود. از آن‌جایی که انجام مطالعات آزمایشگاهی برای بررسی رفتار FCG تحت شرایط مختلف بارگذاری و محیطی وقت‌گیر و پرهزینه است، استفاده از یک روش قابل اطمینان برای پیش‌بینی این رفتار بسیار حائز اهمیت است. دراین‌خصوص یک روش مدلسازی مبتنی بر تکنیک حداقل مربعات ماشین بردار پشتیبان (LSSVM) برای پیش بینی رفتار FCG در سه آلیاژ مختلف شامل یک آلیاژ Ti-6Al-4V و دو فولاد حاوی مس کم آلیاژ و استحکام بالا (HSLA) در دو محیط مختلف هوا و محیط خورنده مورد استفاده قرار گرفت. پارامترهای این مدل با استفاده از روش بهینه‌یابی آنیل شبیه‌سازی شده کوپل محاسبه گردید. همچنین عملکرد و دقت مدل توسعه داده شده با استفاده از قابلیت مدل برای پیش‌بینی داده‌های آزمایشگاهی مورد ارزیابی و صحت‌سنجی قرار گرفت. تحلیل آماری خطا نیز نشان داد که مدل توسعه داده شده می‌تواند داده‌های آزمایشگاهی را با دقت بالایی پیش‌بینی نمایید.

واژه‌های کلیدی: رشد ترک خستگی- خوردگی، مدلسازی، LSSVM، Ti-6Al-4V، فولاد HSLA